

## Article

# Differentiating the Reactivity of ZrO<sub>2</sub>-Bound Formates Formed on Cu/ZrO<sub>2</sub> during CO<sub>2</sub> Hydrogenation

Frederic C. Meunier , Isaac Dansette, Kimleang Eng  and Yves Schuurman 

Institut de Recherches sur la Catalyse et l'Environnement de Lyon, IRCELYON, Université Claude Bernard Lyon 1, Univ Lyon, CNRS, 2 Av. Albert Einstein, 69626 Villeurbanne, France; isaac.dansette@gmail.com (I.D.); engkimleang@hotmail.com (K.E.); yves.schuurman@ircelyon.univ-lyon1.fr (Y.S.)

\* Correspondence: frederic.meunier@ircelyon.univ-lyon1.fr

**Abstract:** The surface species formed during the hydrogenation of CO<sub>2</sub> with H<sub>2</sub> over a ZrO<sub>2</sub>-supported Cu catalyst were investigated by *operando* diffuse reflectance FT-IR spectroscopy at 220 °C and 3 bar. The reactivity of two different formates located on zirconia could be unraveled. The data pointed to ZrO<sub>2</sub> hydroxyl groups at 3755 cm<sup>-1</sup> as the sites on which carbonates and then formates were hydrogenated to methoxy species. Formate hydrogenation appeared as the slowest step. The most reactive ZrO<sub>2</sub>-bound formates exhibited a rate constant of reaction about 65 times higher than that of the slower formate.

**Keywords:** CO; platinum; FT-IR; in situ; *operando*

## 1. Introduction

The hydrogenation of CO<sub>2</sub> to produce methanol enables recycling CO<sub>2</sub> into a base chemical that can also be directly used as a fuel [1–4]. Cu/ZnO/Al<sub>2</sub>O<sub>3</sub> is the reference industrial catalyst for methanol synthesis and has been developed primarily for CO-containing feed [3]. A major difference between using CO (Equation (1)) and using CO<sub>2</sub> (Equation (2)) for manufacturing methanol is the formation of water, which can also be obtained through the reverse water gas-shift reaction (RWGS, Equation (3)):



The increased presence of water in the reactor will impact the long-term stability of Cu/ZnO/Al<sub>2</sub>O<sub>3</sub> catalysts due to the poor hydrothermal stability of alumina. In fact, Prašnikar et al. showed that a correlation existed between alumina surface area and Cu particle sizes during accelerated aging tests [5]. Golunski and Burch [3], stressed the need to stabilize alumina against densification or find a more durable support.

ZrO<sub>2</sub> is a strong candidate to be used as a support for methanol synthesis catalysts because of its well-known hydrothermal stability. The melting point of zirconia is 2715 °C, in comparison to 2072 °C for alumina. ZrO<sub>2</sub>-based catalysts have been successfully used for many demanding reactions such as the dry [6] and steam [7] reforming of methane, steam-reforming of methanol [8] (the reverse reaction of that of interest here) and aqueous-phase reactions in acidic media [9].

Unpromoted ZrO<sub>2</sub> present some activity by itself for CO<sub>2</sub> hydrogenation, its combination with ZnO yield even greater interesting activity, although less than those obtained when combined with Cu [10]. In fact, the combination of Cu and ZrO<sub>2</sub> is one of the most



**Citation:** Meunier, F.C.; Dansette, I.; Eng, K.; Schuurman, Y. Differentiating the Reactivity of ZrO<sub>2</sub>-Bound Formates Formed on Cu/ZrO<sub>2</sub> during CO<sub>2</sub> Hydrogenation. *Catalysts* **2022**, *12*, 793. <https://doi.org/10.3390/catal12070793>

Academic Editor: Catia Cannilla

Received: 29 June 2022

Accepted: 13 July 2022

Published: 19 July 2022

**Publisher's Note:** MDPI stays neutral with regard to jurisdictional claims in published maps and institutional affiliations.



**Copyright:** © 2022 by the authors. Licensee MDPI, Basel, Switzerland. This article is an open access article distributed under the terms and conditions of the Creative Commons Attribution (CC BY) license (<https://creativecommons.org/licenses/by/4.0/>).

efficient to obtain high reaction rates to methanol with CO/CO<sub>2</sub>/H<sub>2</sub> [3,11] or CO<sub>2</sub>/H<sub>2</sub> mixture [12–15] Cu supported on amorphous zirconia was found to be more active than the catalysts made from monoclinic or tetragonal polymorphs, though ageing was not considered [16].

Numerous IR studies have been reported on the Cu-catalyzed hydrogenation of CO [17,18] and CO<sub>2</sub> [19–23] to methanol, with formates often proposed as being a main reaction intermediate. Fischer and Bell investigated the hydrogenation of CO<sub>2</sub> over Cu/ZrO<sub>2</sub>/SiO<sub>2</sub> and proposed that Cu favored the activation of H<sub>2</sub> that spilled over to ZrO<sub>2</sub> to promote carbonate/hydrogenocarbonate hydrogenation into formates and then to methoxide species [21].

The role of formates in the hydrogenation of CO<sub>2</sub> over ZrO<sub>2</sub>-supported Cu has actually been the subject of a controversy. Two distinct pathways have been proposed (Figure 1). Kattel et al. [22] proposed a formate-free pathway, starting with the reverse WGS (RWGS) and the formation of a CO-OH hydroxycarbonyl intermediate. In contrast, Larmier et al. [24] proposed a formate-based route, in which a ZrO<sub>2</sub>-bound formate located at the interface with Cu nanoparticles is hydrogenated by H<sub>2</sub> activated on Cu to methoxy, still on the support.

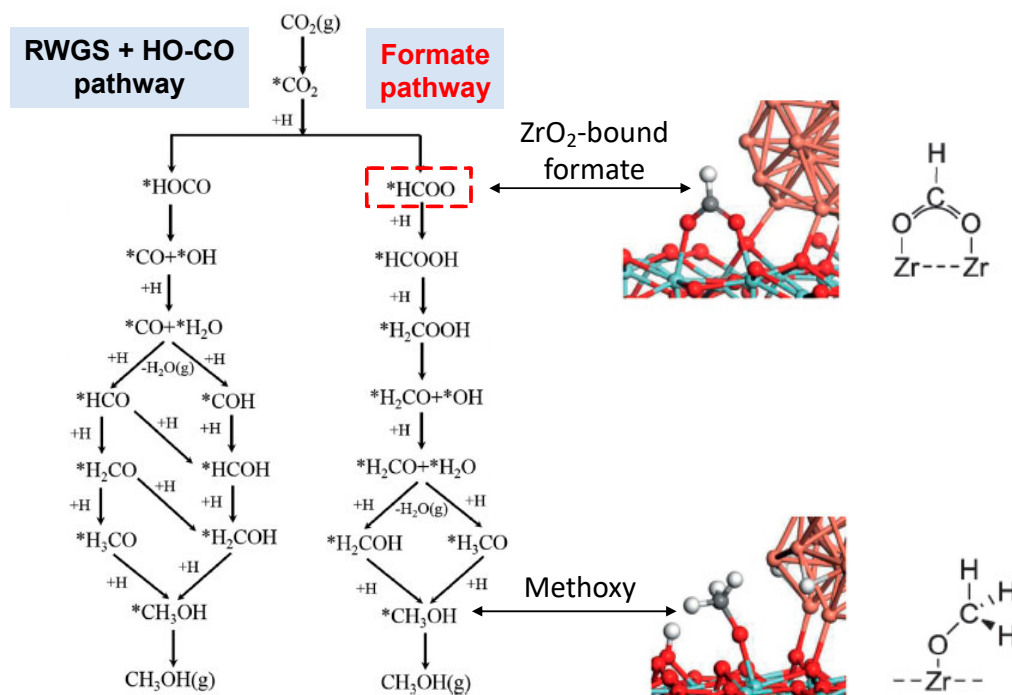


**Figure 1.** Reaction pathways proposed on Cu/ZrO<sub>2</sub>. (Adapted from reference [22], Kattel et al. J. Am. Chem. Soc. 138 (2016) 12440–12450 with permission, © 2016 American Chemical Society and from reference [24], Larmier et al., Angew Chem. Int. Ed. Angew. Chem. Int. Ed. 2017, 56, 2318–2323 © 2017 Wiley-VCH Verlag GmbH & Co. KGaA, Weinheim). The \* symbol indicates an adsorbed species.

We have previously investigated formate decomposition over alumina-supported cobalt used for CO hydrogenation [25]. The reactivity of formates was determined by inducing a chemical transient, i.e., by removing CO from the feed. Interestingly, two types of formate reactivity were observed, despite the fact that both formate species exhibited identical DRIFTS spectra. These facts were rationalized by proposing that the reactivity of these alumina-bound formates differed depending on their proximity to the alumina-metal interface.

A similar experimental approach has been used here to investigate the hydrogenation of CO<sub>2</sub> over a zirconia-supported Cu catalyst. The present work aims at highlighting different types of formate species present at the surface of the catalyst and their relative reactivity.

## 2. Experimental Section

A 6 wt.% Cu/ZrO<sub>2</sub> catalyst was prepared by incipient wetness impregnation of zirconia (from MEL Chemicals, monoclinic, 131 m<sup>2</sup> g<sup>-1</sup>) using Cu(NO<sub>3</sub>)<sub>2</sub> · 6 H<sub>2</sub>O. The impregnated sample was then dried at room temperature for 24 h before being oven-dried at 110 °C for 12 h. The sample was finally calcined at 450 °C for 12 h in synthetic flowing air. The sample was reduced in situ at 350 °C under flowing 80% H<sub>2</sub>/He for 1 h before the CO<sub>2</sub> hydrogenation experiments.

Copper dispersion was measured using N<sub>2</sub>O titration (frontal chromatography) using a 10 cm-pathlength FT-IR gas cell as detector. The sample was reduced in situ at 300 °C in 50% H<sub>2</sub>/He for 1 h, purge in He and brought to 75 °C to be exposed to 2000 ppm of N<sub>2</sub>O in a flow rate of 36 mL min<sup>-1</sup>. It was assumed that each O deposited on the surface titrated two Cu surface atoms [26,27].

Powder X-ray diffraction patterns (XRD) were recorded to assess the crystallinity of the samples. Diffractograms were collected between 10 and 80° (2 $\theta$ ) with steps of 0.02° and 1 s per step with a Bruker D8-Advance diffractometer using CuK $\alpha$  radiation at  $\lambda$  = 1.5418 Å. Nitrogen adsorption isotherms were measured at 77 K on an ASAP 2020 from Micromeritics. Samples were first outgassed under vacuum at 300 °C for 3 h.

High-purity gases He, CO, CO<sub>2</sub> and H<sub>2</sub> from Air Liquid were used for the *operando* catalytic tests. The experiments were carried out at 3 bars using a mixture of 20% CO<sub>2</sub> + 60% H<sub>2</sub> in He at a total flowrate of 75 mL min<sup>-1</sup>, unless otherwise stated. *Operando* DRIFTS experiments were performed on a modified high-temperature DRIFT cell (from Spectra-Tech, Hong Kong) fitted with CaF<sub>2</sub> windows using a Collector II assembly. A description and properties of the cell can be found in earlier references [28–30]. The spectrophotometer used was a Nicolet 8700 (ThermoFischer Scientific, Waltham, MA, USA) fitted with a liquid-N<sub>2</sub> cooled MCT detector. The DRIFT spectra were recorded at a resolution of 4 cm<sup>-1</sup> and 8 scans were averaged. The DRIFTS spectra are reported as log (1/R), where R is the sample reflectance. This pseudo-absorbance gives a better linear representation of the band intensity against surface coverage than that given by the Kubelka–Munk function for strongly absorbing media such as those based on metals supported on oxides [31]. The contribution of gas-phase CO was subtracted using a CO(g) spectrum collected under the same experimental conditions over KBr powder [32,33].

The reaction products were analyzed using a transmission FT-IR gas-cell (200 mL dead-volume) with a 2 m pathlength kept at 60 °C to prevent product condensation. The pressure in the system was controlled by a back-pressure regulator located after the DRIFTS cell and before the transmission FT-IR gas cell. The pressure in the line was precisely measured using an electronic gauge.

## 3. Results and Discussion

The surface area of the calcined 6 wt.% Cu/ZrO<sub>2</sub> catalyst was 123 m<sup>2</sup> g<sup>-1</sup>. The sample exhibited a Cu surface area measured by N<sub>2</sub>O frontal chromatography of about 8.3 m<sup>2</sup> g<sup>-1</sup>, corresponding to Cu spherical particles with an average diameter of 4.9 nm. In view of these two surface measurements, it can be concluded that the ZrO<sub>2</sub> surface represented the largest fraction (ca. 93%) of the surface area of the sample.

The diffraction patterns of the ZrO<sub>2</sub> support and Cu/ZrO<sub>2</sub> sample showed the presence of mostly monoclinic zirconia with traces of a tetragonal phase (Figure 2A). Very weak and broad peaks associated with CuO were also observed in the case of the calcined Cu/ZrO<sub>2</sub> sample, which are consistent with the high dispersion of the Cu phase determined through N<sub>2</sub>O titration.

The in situ spectrum at 220 °C of the Cu/ZrO<sub>2</sub> sample reduced at 350 °C prior to exposure to the feed (Figure 2B, Red) showed two main broad bands at about 3755 and 3665 cm<sup>-1</sup> typical of zirconia surface hydroxyl groups [34]. A group of bands near 1505 cm<sup>-1</sup> was also observed, indicated the residual presence of strongly bound carbonates that were not decomposed during the reduction step.

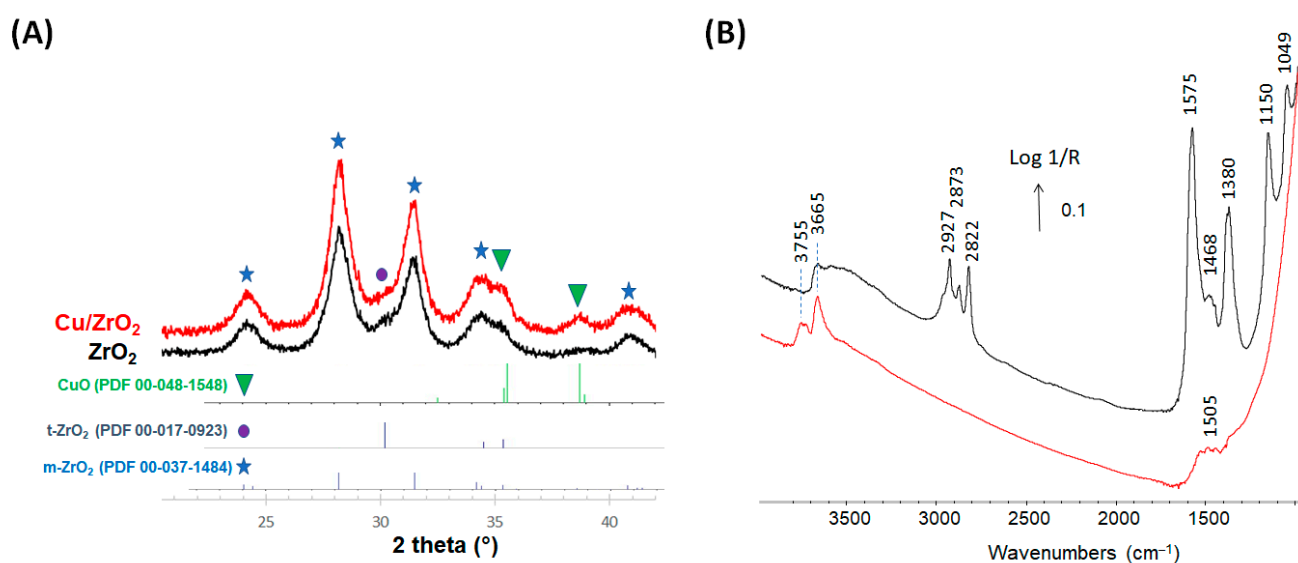


**Figure 2.** (A) XRD patterns of the zirconia support and the calcined zirconia-supported Cu. The main peaks of PDF reference files are given underneath. (B) In situ DRIFTS spectrum at 220 °C of the ZrO<sub>2</sub>-supported Cu sample under 80% H<sub>2</sub>/He (Red) after reduction at 350 °C and (Black) after reaction and then exposed to H<sub>2</sub>-only feed for 60 min at 220 °C.

Methanol and CO were the only C-containing products observed at 220 °C and 3 bar when the 20% CO<sub>2</sub> + 60% H<sub>2</sub> feed was introduced. A steady state was achieved within one hour on stream in terms of methanol and CO concentrations measured at the exit of the DRIFTS cell and in terms of DRIFTS signals of the various adsorbates observed. Differential conditions were obtained with a CO<sub>2</sub> conversion of about 0.8%. The selectivity to methanol was about 47%, and the productivity was 1.0 μmol(CH<sub>3</sub>OH) s<sup>-1</sup> g<sub>Catalyst</sub><sup>-1</sup>. These values are similar to those reported by Fischer and Bell [21] at 250 °C and 6.5 bar for a Cu/ZrO<sub>2</sub>/SiO<sub>2</sub>, that were 1.3 μmol(CH<sub>3</sub>OH) s<sup>-1</sup> g<sub>Catalyst</sub><sup>-1</sup> and a selectivity to methanol of 43%. The operando spectrum obtained at steady state under the CO<sub>2</sub> and H<sub>2</sub> feed at 220 °C is shown in Figure 3A (top). The set of bands at 2873, 1575 and 1380 cm<sup>-1</sup> corresponded to formate species [35,36], mostly, if not wholly, adsorbed on the zirconia support (Table 1). The band around 1468 cm<sup>-1</sup> can be assigned to polydentate carbonates formed from CO<sub>2</sub> adsorption on zirconia basic sites [21]. The bands at 2927, 2822, 1150 and 1049 cm<sup>-1</sup> were assigned to methoxy groups [34,37]. The methoxy species with the band at 1150 cm<sup>-1</sup> (corresponding to the stretching C-O vibration ν(O-C)) was proposed to be formed over zirconia hydroxyl groups located near 3755 cm<sup>-1</sup> and be a monodentate species. In contrast, the methoxy with a band at 1049 cm<sup>-1</sup> was proposed to derive from the adsorption on the site associated with hydroxyl groups at 3665 cm<sup>-1</sup> and be a bridged methoxy [34,37].

Interestingly, no evidence of CO adsorbed on Cu was apparent. To assess whether or not adsorbed CO could ever be observed, an experiment was carried out replacing CO<sub>2</sub> with CO. A large band centered around 2010 cm<sup>-1</sup> assigned to CO adsorbed on metallic copper [38] was observed when CO was used (Figure 3A (bottom)). This indicates that the coverage of the Cu nanoparticles is very different in the presence of CO<sub>2</sub>, as compared to the case of CO. More work would be needed to determine the nature of the main species covering the Cu surface in this case (e.g., H, O). It is interesting to note that, apart from the CO(ads) signal, the rest of the spectra was almost identical, pointing to similar coverages of methoxy, formates and carbonates over the ZrO<sub>2</sub> support whether CO or CO<sub>2</sub> were used.

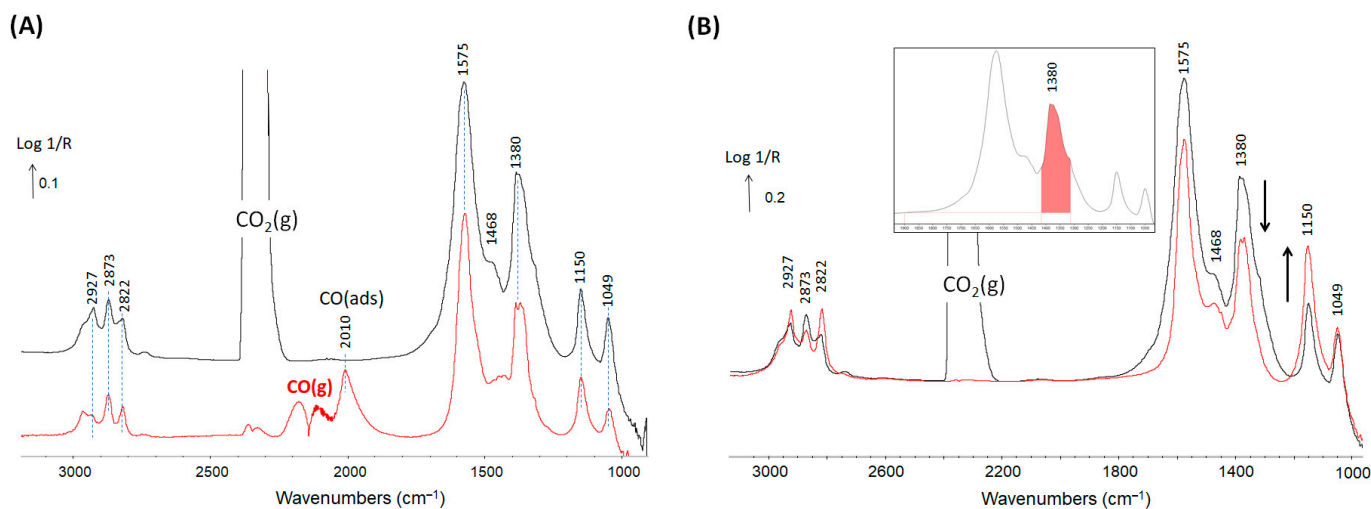


**Figure 3.** (A) *Operando* DRIFTS spectra collected at steady state 220 °C and 3 bar under (black, top) 20% CO<sub>2</sub> + 60% H<sub>2</sub> and (red, bottom) 25% CO + 75% H<sub>2</sub>. (B) (Black) same as (A, black, top) and (Red) in situ DRIFTS spectra collected at 220 °C and 3 bar under H<sub>2</sub>/He after having removed CO<sub>2</sub> from the feed for 60 min. Inset: region used to integrate the formate signal.

**Table 1.** Tentative IR band assignments.

Wavenumber (cm <sup>-1</sup> )	References
3755 and 3665	Hydroxyls on zirconia [34]
2873, 1575 and 1380	Formate on zirconia [35,36]
1468	Multi-bonded carbonates [21]
2927, 2822, 1150	Methoxy type I [34,37]
2927, 2822, 1049	Methoxy type II [34,37]
2010	carbonyl on Cu <sup>0</sup> [38]

CO<sub>2</sub> was removed from the feed, and the spectrum obtained after 60 min in H<sub>2</sub> at 220 °C is shown in Figure 3B and compared to the steady-state spectrum. The carbonate and formate signals decreased significantly, while that of the methoxy at 1150 cm<sup>-1</sup> increased. In contrast, the methoxy at 1049 cm<sup>-1</sup> remained essentially unchanged. These observations show first that all the surface species were bound rather strongly to the surface and were poorly reactive under H<sub>2</sub> at 220 °C, all likely bound to ZrO<sub>2</sub> sites. The data also suggest that a fraction of carbonates and formates had been converted into the methoxy at 1150 cm<sup>-1</sup>. These results would suggest that zirconia hydroxyl groups at 3755 cm<sup>-1</sup>, associated with the 1150 cm<sup>-1</sup> methoxy, are the location at which carbonate and formate species are hydrogenated to methoxy. Bensitel et al. [34] had actually reported that only the 3755 cm<sup>-1</sup> hydroxyl species reacted with CO<sub>2</sub> to form hydrogenocarbonate species, stressing the unique reactivity of this site.

The decay of the signal in the formate region was investigated by integrating over the range 1415.5–1313.1 cm<sup>-1</sup>, using a single point baseline located at 1900 cm<sup>-1</sup> (see inset in Figure 3B). The signal decay in the first minute was quite complex, consisting of a rapid evolution of overlapping increasing and decreasing contributions, and will be dealt with in a subsequent contribution.

The signal decay in the time range 1–60 min is presented in Figure 4. The total signal could be decomposed into a slow linear contribution and a faster decay (Figure 4A). A semi-logarithmic plot of the faster signal decay showed a linear behavior, indicating a uniform reactivity (Figure 4B). The difference DRIFTS spectrum obtained by subtracting the spectra collected after having removed CO<sub>2</sub> for 2 min and 20 min, when most of the fast signal

species had gone, is shown in Figure 5. It shows that the lost signal corresponding to this fast-removed species was essentially a formate similar to that prevailing at steady state. The larger band width observed was possibly due to a larger distribution of heterogeneous sites. The slow remaining species left after more than 30 min under H<sub>2</sub> was already discussed above (Figure 3B) and also corresponded to ZrO<sub>2</sub>-bound formates.

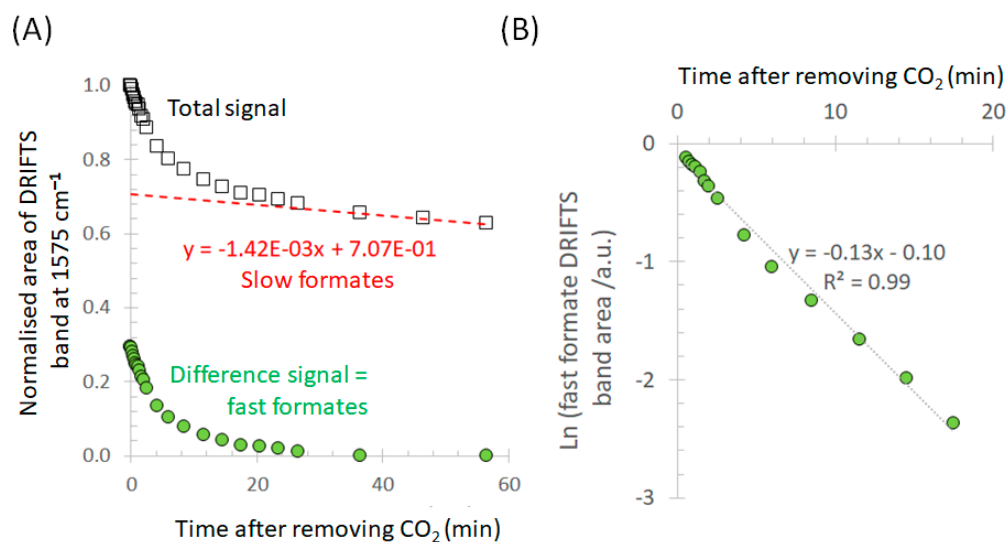


**Figure 4.** (A) Evolution of DRIFTS band area recorded over Cu/ZrO<sub>2</sub> at 220 °C as a function of time under 85% H<sub>2</sub> in He. The time range 1–60 min is presented. The total signal (open square) could be decomposed into a slow linear contribution (red dotted line) and a faster decay (green circles). Total flow = 100 mL min<sup>-1</sup>. (B) Semi-logarithmic plot of the normalized signal associated with the faster decay showing a linear behavior.

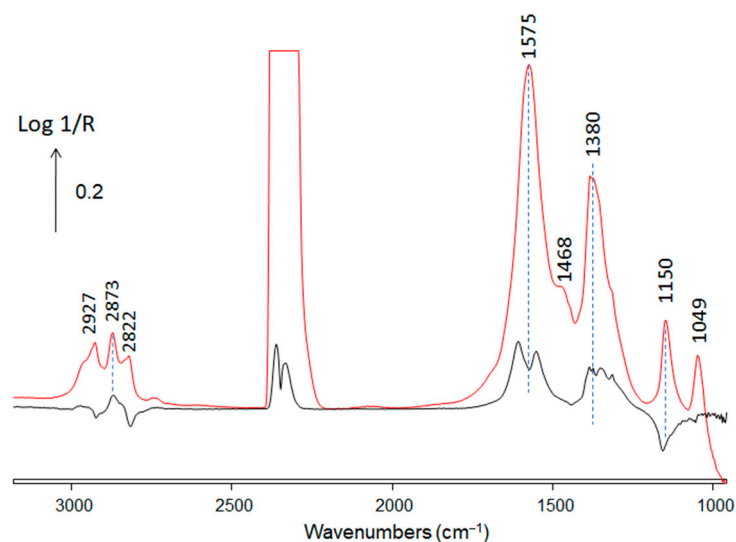


**Figure 5.** Operando DRIFTS spectra collected (Red) at steady state under CO<sub>2</sub> + H<sub>2</sub> at 220 °C and (Black) difference between the spectra collected after 2 and 20 min after having removed CO<sub>2</sub> from the feed.

The rate constant of reaction/decomposition of the two normalized signals of the so-called “slow” and “fast” formates on ZrO<sub>2</sub> were approximately equal to  $2 \times 10^{-3} \text{ min}^{-1}$  and  $1.3 \times 10^{-1} \text{ min}^{-1}$ , respectively. The fast formate thus exhibited a ca. 65-fold higher reactivity than the slow formate. It must be stressed here that the products (adsorbed or gas-phase) to which these formates decomposed into could not be directly measured.

The evolution of the methoxy DRIFTS band area at  $1150\text{ cm}^{-1}$  was plotted as a function of those of the total formate band (Figure 6A) and fast formate-only band (Figure 6B) following the removal of  $\text{CO}_2$ . These plots show that a strong correlation existed between these quantities, primarily the fast formate band (since the slow formate hardly changed over the duration of the experiment) and the methoxy at  $1150\text{ cm}^{-1}$ . This quantitative correlation supports the aforementioned model that the  $\text{ZrO}_2$  hydroxyl groups at  $3755\text{ cm}^{-1}$ , on which the  $1150\text{ cm}^{-1}$  methoxy is formed, were the sites where carbonates and then formates were hydrogenated to methoxy species. It is interesting to note that the  $3755\text{ cm}^{-1}$  hydroxyl group was still totally missing after 60 min exposure to  $\text{H}_2$  at  $220\text{ }^\circ\text{C}$  (Figure 2B, Black), indicating that those were still involved in bonding some adsorbates (formates or methoxy).

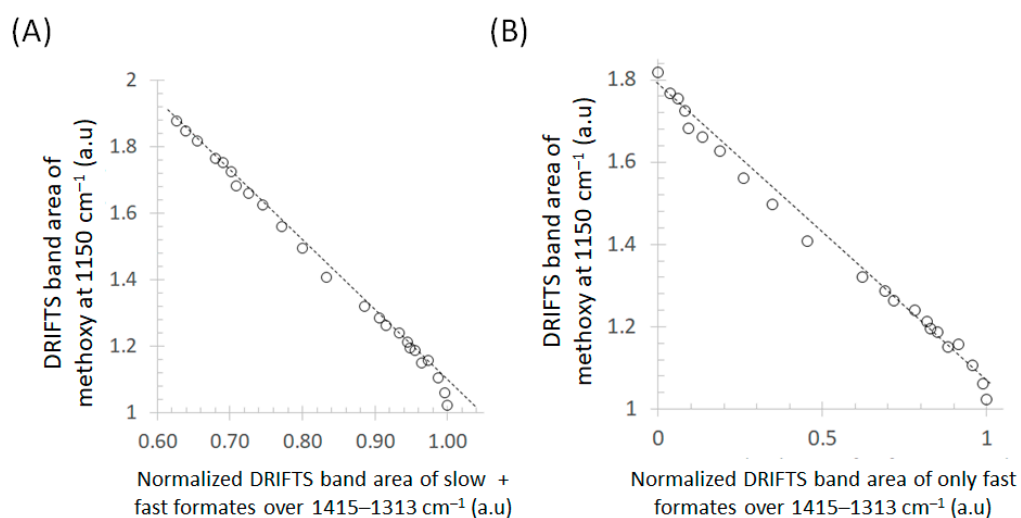


**Figure 6.** Variation of the methoxy DRIFTS band area at  $1150\text{ cm}^{-1}$  as a function of that of the formate band following the removal of  $\text{CO}_2$ . Feed:  $100\text{ mL min}^{-1}$  of  $85\%\text{ H}_2/\text{He}$ .

The findings here are consistent with a reaction model in which carbonates formed from  $\text{CO}_2$  adsorption on zirconia are readily reduced to formate species. The hydrogenation of formates to methoxy is then kinetically limiting, explaining the large signal of formate species. These steps are all favored by  $\text{H}_2$  activation over Cu followed by spillover of H onto the support, as proposed earlier by Fisher and Bell [21]. The accumulation of methoxy species may also occur, if methanol readsorption is significant and if the reductive elimination or hydrolysis of methoxy groups is slow. Fisher and Bell have actually observed of a similar sample that methoxy hydrolysis (by water formed in the reaction) was significantly faster than reductive elimination [21]. This may explain the accumulation of methoxy species in conditions under which water production is limited or totally absent, as in the present case under the  $\text{H}_2/\text{He}$  stream.

Some of the main findings obtained here are summarized in Figure 7. Formate species are observed under reactions conditions that are mostly  $\text{ZrO}_2$ -bound. The reactivity of  $\text{ZrO}_2$ -bound formates is two-fold, with a fast formate exhibiting a rate constant of decomposition 65 times higher than that of a slower formate species. The fast formate species appears to be hydrogenated into methoxy groups that are associated with  $\text{ZrO}_2$  hydroxyl groups at  $3755\text{ cm}^{-1}$ . It is not yet clear if the hydrogenation ability is solely related to the nature of the zirconia sites or if the distance to the copper–zirconia interface matters, for instance, as a result of H-spillover. It is possible that the slow formates were located on domains or  $\text{ZrO}_2$  crystallites on which no Cu nanoparticles were present and thus almost no spillover H would be available. On the contrary, the fast formates could be located on  $\text{ZrO}_2$  crystals on which Cu nanoparticles would be present and spillover H would be readily available, enabling a uniform reactivity of formates on such domains.

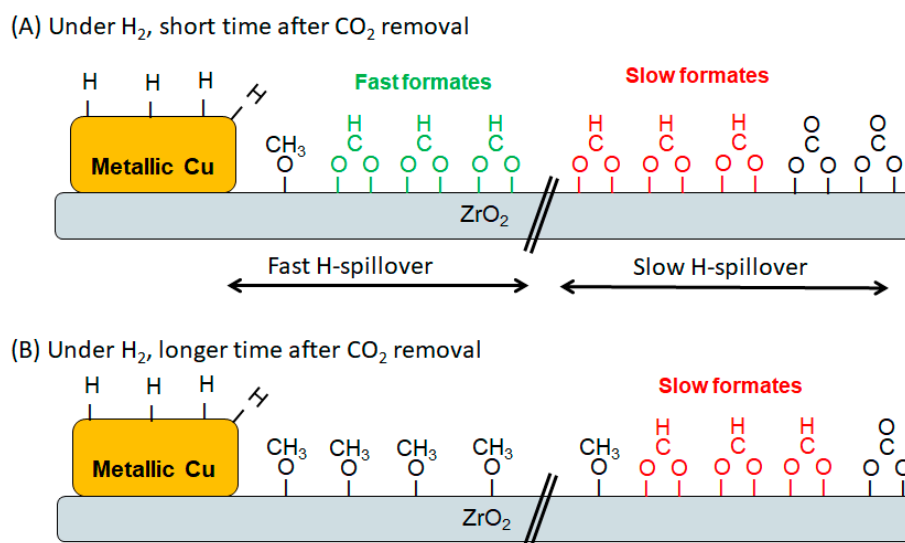


**Figure 7.** Schematic representation of the evolution of the  $ZrO_2$ -bound formates under  $H_2$ . See text for more details.

#### 4. Conclusions

This contribution reveals that on a zirconia-supported copper catalyst used for  $CO_2$  hydrogenation, two main types of zirconia-bound formates are present. A significant difference in reactivity is observed (ca. 65-fold), partly related to the nature of the hydroxyl group on which these formates are adsorbed. More work is under way to quantitatively relate the rate of formation of methanol to the reaction rate of the formate species present over zirconia.

**Author Contributions:** F.C.M. conceptualized the work. F.C.M. and K.E. carried out the IR analyses. I.D. carried out the  $N_2O$ -TPD and XRD analyses. F.C.M. prepared the draft of the paper and all authors contributed to the final version. Validation: Y.S.; Writing–review & editing: Y.S. The manuscript was written through contributions of all authors. All authors have read and agreed to the published version of the manuscript.

**Funding:** This research received no external funding.

**Institutional Review Board Statement:** Not applicable.

**Conflicts of Interest:** The authors declare no conflict of interest.

#### References

- Meunier, F.C. Mixing Copper Nanoparticles and ZnO Nanocrystals: A Route towards Understanding the Hydrogenation of  $CO_2$  to Methanol? *Angew. Chem. Int. Ed.* **2011**, *50*, 4053–4054. [[CrossRef](#)] [[PubMed](#)]
- Bowker, M. Methanol Synthesis from  $CO_2$  Hydrogenation. Methanol Synthesis from  $CO_2$  Hydrogenation. *ChemCatChem* **2019**, *11*, 4238–4246. [[CrossRef](#)] [[PubMed](#)]
- Golunski, S.; Burch, R.  $CO_2$  Hydrogenation to Methanol over Copper Catalysts: Learning from Syngas Conversion. *Top. Catal.* **2021**, *64*, 974–983. [[CrossRef](#)]
- Jiang, X.; Nie, X.; Guo, X.; Song, C.; Chen, J.G. Recent Advances in Carbon Dioxide Hydrogenation to Methanol via Heterogeneous Catalysis. *Chem. Rev.* **2020**, *120*, 7984–8034. [[CrossRef](#)]
- Pavlišič, P.A.; Ruiz-Zepeda, F.; Kovač, J.; Likozar, B. Mechanisms of Copper-Based Catalyst Deactivation during  $CO_2$  Reduction to Methanol. *Ind. Eng. Chem. Res.* **2019**, *58*, 13021–13029.
- O'Connor, A.M.; Meunier, F.C.; Ross, J.R.H. An In-situ DRIFTS Study of the Mechanism of the  $CO_2$  Reforming of  $CH_4$  over a Pt/ $ZrO_2$  Catalyst. *Stud. Surf. Sci. Catal.* **1998**, *119*, 819–824.
- Lim, Z.-Y.; Wu, C.Z.; Wang, W.G.; Choy, K.-L.; Yin, H. Porosity effect on  $ZrO_2$  hollow shells and hydrothermal stability for catalytic steam reforming of methane. *J. Mater. Chem. A* **2016**, *4*, 153–159. [[CrossRef](#)]
- Breen, J.P.; Meunier, F.C.; Ross, J.R.H. Mechanistic aspects of the steam reforming of methanol over a CuO/ $ZnO$ / $ZrO_2$ / $Al_2O_3$  catalyst. *Chem. Commun.* **1999**, *22*, 2247–2248. [[CrossRef](#)]

9. Al-Naji, M.; Popova, M.; Chen, Z.; Wilde, N.; Glaser, R. Aqueous-Phase Hydrogenation of Levulinic Acid Using Formic Acid as a Sustainable Reducing Agent Over Pt Catalysts Supported on Mesoporous Zirconia. *ACS Sust. Chem. Eng.* **2020**, *8*, 393–402. [[CrossRef](#)]
10. Wang, J.; Li, G.; Li, Z.; Tang, C.; Feng, Z.; An, H.; Liu, H.; Liu, T.; Li, C. A highly selective and stable ZnO-ZrO<sub>2</sub> solid solution catalyst for CO<sub>2</sub> hydrogenation to methanol. *Sci. Adv.* **2017**, *3*, e1701290. [[CrossRef](#)]
11. Burch, R.; Golunski, S.E.; Spencer, M.S. The role of copper and zinc oxide in methanol synthesis catalysts. *J. Chem. Soc. Faraday Trans.* **1990**, *86*, 2683–2691. [[CrossRef](#)]
12. Arena, F.; Barbera, K.; Italiano, G.; Bonura, G.; Spadaro, L.; Frusteri, F. Synthesis, characterization and activity pattern of Cu–ZnO/ZrO<sub>2</sub> catalysts in the hydrogenation of carbon dioxide to methanol. *J. Catal.* **2007**, *249*, 185–194. [[CrossRef](#)]
13. Arena, F.; Italiano, G.; Barbera, K.; Bordiga, S.; Bonura, G.; Spadaro, L.; Frusteri, F. Solid-state interactions, adsorption sites and functionality of Cu–ZnO/ZrO<sub>2</sub> catalysts in the CO<sub>2</sub> hydrogenation to CH<sub>3</sub>OH. *Appl. Catal. A Gen.* **2008**, *350*, 16–23. [[CrossRef](#)]
14. Amenomiya, Y. Methanol synthesis from CO<sub>2</sub> + H<sub>2</sub> II. Copper-based binary and ternary catalysts. *Appl. Catal.* **1987**, *30*, 57–68. [[CrossRef](#)]
15. Li, K.; Chen, J.G. CO<sub>2</sub> Hydrogenation to Methanol over ZrO<sub>2</sub>-Containing Catalysts: Insights into ZrO<sub>2</sub> Induced Synergy. *ACS Catal.* **2019**, *9*, 7840–7861. [[CrossRef](#)]
16. Tada, S.; Kayamori, S.; Honma, T.; Kamei, H.; Nariyuki, A.; Kon, K.; Toyao, T.; Shimizu, K.-I.; Satokawa, S. Design of Interfacial Sites between Cu and Amorphous ZrO<sub>2</sub> Dedicated to CO<sub>2</sub>-to-Methanol Hydrogenation. *ACS Catal.* **2018**, *8*, 7809–7819. [[CrossRef](#)]
17. Fisher, I.A.; Bell, A.T. In Situ Infrared Study of Methanol Synthesis from H<sub>2</sub>/CO over Cu/SiO<sub>2</sub> and Cu/ZrO<sub>2</sub>/SiO<sub>2</sub>. *J. Catal.* **1998**, *178*, 153–173. [[CrossRef](#)]
18. Rhodes, M.D.; Pokrovski, K.A.; Bell, A.T. The effects of zirconia morphology on methanol synthesis from CO and H<sub>2</sub> over Cu/ZrO<sub>2</sub> catalysts: Part II. Transient-response infrared studies. *J. Catal.* **2005**, *233*, 210–220. [[CrossRef](#)]
19. Fujita, S.-I.; Usui, M.; Ohara, E.; Takezawa, N. Methanol synthesis from carbon dioxide at atmospheric pressure over Cu/ZnO catalyst. Role of methoxide species formed on ZnO support. *Catal. Lett.* **1992**, *13*, 349–358. [[CrossRef](#)]
20. Millar, G.J.; Rochester, C.H.; Waugh, K.C. An in situ high pressure FT-IR study of CO<sub>2</sub>/H<sub>2</sub> interactions with model ZnO/SiO<sub>2</sub>, Cu/SiO<sub>2</sub> and Cu/ZnO/SiO<sub>2</sub> methanol synthesis catalysts. *Catal. Lett.* **1992**, *14*, 289–295. [[CrossRef](#)]
21. Fisher, I.A.; Bell, A.T. In Situ Infrared Study of Methanol Synthesis from H<sub>2</sub>/CO<sub>2</sub> over Cu/SiO<sub>2</sub> and Cu/ZrO<sub>2</sub>/SiO<sub>2</sub>. *J. Catal.* **1997**, *172*, 222–237. [[CrossRef](#)]
22. Kattel, S.; Yan, B.; Yang, Y.; Chen, J.G.; Liu, P. Optimizing Binding Energies of Key Intermediates for CO<sub>2</sub> Hydrogenation to Methanol over Oxide-Supported Copper. *J. Am. Chem. Soc.* **2016**, *138*, 12440–12450. [[CrossRef](#)] [[PubMed](#)]
23. Lam, E.; Corral-Pérez, J.J.; Larmier, K.; Noh, G.; Wolf, P.; Comas-Vives, A.; Urakawa, A.; Copéret, C. CO<sub>2</sub> Hydrogenation on Cu/Al<sub>2</sub>O<sub>3</sub>: Role of the Metal/Support Interface in Driving Activity and Selectivity of a Bifunctional Catalyst. *Angew. Chem. Int. Ed.* **2019**, *58*, 13989–13996. [[CrossRef](#)] [[PubMed](#)]
24. Larmier, K.; Liao, W.C.; Tada, S.; Lam, E.; Verel, R.; Bansode, A.; Urakawa, A.; Comas-Vives, A.; Copéret, C. CO<sub>2</sub>-to-Methanol Hydrogenation on Zirconia-Supported Copper Nanoparticles: Reaction Intermediates and the Role of the Metal–Support Interface. *Angew. Chem. Int. Ed.* **2017**, *56*, 2318–2323. [[CrossRef](#)]
25. Paredes-Nunez, L.A.; Mirodatos, C.; Schuurman, Y.; Meunier, F.C. Determination of formate decomposition rates and relation to product formation during CO hydrogenation over supported cobalt. *Catal. Today* **2015**, *259*, 192–196.
26. Chinchén, G.C.; Hay, C.M.; Vandervell, H.D.; Waugh, K.C. The measurement of copper surface areas by reactive frontal chromatography. *J. Catal.* **1987**, *103*, 79–86. [[CrossRef](#)]
27. Bennici, G.S. Dispersion and surface states of copper catalysts by temperature-programmed-reduction of oxidized surfaces (s-TPR). *Appl. Catal. A Gen.* **2005**, *281*, 199–205.
28. Meunier, F.C.; Goguet, A.; Shekhtman, S.; Rooney, D.; Daly, H. A modified commercial DRIFTS cell for kinetically relevant operando studies of heterogeneous catalytic reactions. *Appl. Catal. A Gen.* **2008**, *340*, 196–202. [[CrossRef](#)]
29. Li, H.; Rivallan, M.; Thibault-Starzyk, F.; Travert, A.; Meunier, F.C. Effective bulk and surface temperatures of the catalyst bed of FT-IR cells used for in situ and operando studies. *Phys. Chem. Chem. Phys.* **2013**, *5*, 7321–7327. [[CrossRef](#)]
30. Bredy, P.; Farrusseng, D.; Schuurman, Y.; Meunier, F.C. On the link between CO surface coverage and selectivity to CH<sub>4</sub> during CO<sub>2</sub> hydrogenation over supported cobalt catalysts. *J. Catal.* **2022**, *411*, 93–96. [[CrossRef](#)]
31. Sirita, J.; Phanichphant, S.; Meunier, F.C. Quantitative Analysis of Adsorbate Concentrations by Diffuse Reflectance FT-IR. *Anal. Chem.* **2007**, *79*, 3912–3918. [[CrossRef](#)] [[PubMed](#)]
32. Jbir, P.I.; Bianchi, D.; Meunier, F.C. Spectrum baseline artefacts and correction of gas-phase species signal during diffuse reflectance FT-IR analyses of catalysts at variable temperatures. *Appl. Catal. A Gen.* **2015**, *495*, 17–22.
33. Meunier, F.C. Pitfalls and benefits of in situ and operando diffuse reflectance FT-IR spectroscopy (DRIFTS) applied to catalytic reactions. *React. Chem. Eng.* **2016**, *1*, 134–141. [[CrossRef](#)]
34. Bensitel, M.; Moravek, V.; Lamotte, J.; Saur, O.; Lavalley, J.C. Infrared study of alcohols adsorption on zirconium oxide: Reactivity of alkoxy species towards CO<sub>2</sub>. *Spectrochim. Acta* **1987**, *43*, 1487–1491. [[CrossRef](#)]
35. Busca, G.; Lamotte, J.; Lavalley, J.C.; Lorenzelli, V. FT-IR study of the adsorption and transformation of formaldehyde on oxide surfaces. *J. Am. Chem. Soc.* **1987**, *109*, 5197–5202. [[CrossRef](#)]
36. Meunier, T.F.C.; Goguet, A.; Reid, D.; Burch, R.; Boaro, M.; Vicario, M.; Trovarelli, A. An investigation of possible mechanisms for the water–gas shift reaction over a ZrO<sub>2</sub>-supported Pt catalyst. *J. Catal.* **2006**, *244*, 183–191.

- 
37. Binet, C.; Daturi, M. Methanol as an IR probe to study the reduction process in ceria–zirconia mixed compounds. *Catal. Today* **2001**, *70*, 155–167. [[CrossRef](#)]
  38. Courtois, D.X.; Perrichon, V.; Bianchi, D. Heats of Adsorption of CO on a Cu/Al<sub>2</sub>O<sub>3</sub> Catalyst Using FTIR Spectroscopy at High Temperatures and under Adsorption Equilibrium Conditions. *J. Phys. Chem. B* **2000**, *104*, 6001–6011.